Quasi-Optical Grill Launching of Lower-Hybrid Waves for a Linearly Increasing Plasma Density

Riccardo Borghi, Fabrizio Frezza, *Senior Member, IEEE,* Giorgio Gerosa, *Life Associate Member, IEEE,* Massimo Santarsiero, Carlo Santini, and Giuseppe Schettini, *Member, IEEE*

***Abstract*—An analysis of quasi-optical grills for lower-hybrid waves for heating and current drive purposes is presented. The tokamak plasma density versus the abscissa entering the plasma is assumed to behave like a step and a subsequent ramp. The study is performed by means of a two-dimensional formulation employing cylindrical waves. A detailed numerical analysis is presented, which allows us to show results for different configurations useful in practical cases and comparisons with the constant-density case.**

***Index Terms*— Cylinders, cylindrical arrays, electromagnetic coupling, electromagnetic launching, electromagnetic scattering, plasma heating, plasma waves.**

I. Introduction

As is well known, mechanisms currently used to couple radiofrequency radiation to lower-hybrid plasma waves for heating and current-drive purposes make essential use of evanescent waves [1]. Waveguide grills [2] are presently the most widely used devices in toroidal plasmas, due to the very high flexibility regarding both the launched spectrum and the antenna directivity. However, thousands of waveguides are needed for next-step devices (like International Theormonuclear Experimental Reactor) with obvious handling problems.

In recent years, many alternative solutions have been proposed and developed to simplify the layout and the operation of the coupling structure. Among them, we recall the multijunction [3], which subsequently gave rise to the hyperguide [4], and the quasi-optical grills [5]. In the latter structures the excitation of the plasma lower-hybrid wave is produced by means of the scattering of a radiofrequency beam by a grating of conducting rods, with a drastic reduction in dissipation and complexity of the coupling structure.

The analysis of the coupling of a plane wave, propagating in a vacuum, with a lower hybrid plasma wave by means of a quasi-optical grill, for nuclear fusion purposes, has been tackled with different techniques [3], [5]–[7], giving results in agreement especially for single-line gratings.

In a previous paper [6] we studied the scattering problem of a plane wave by a set of perfectly conducting circular cylinders placed close to a plasma interface. We presented a full-wave solution and gave numerical results for the case of a constant-density plasma, which is simpler from a numerical point of view [8], [9], though important to have estimates of the coupling parameters. In this paper, we intend to extend the results presented there to the case of a linearly-increasing plasma density, which represents a more realistic model [9], [10].

The general lines of the method, briefly recalled in Section II, closely follow those of [6] and [11]. The main novelty presented here, i.e., the treatment of a linearly-increasing plasma density, is made possible by the development of fast and accurate integration methods for the highly oscillating functions involved in the problem. In Section III numerical results are presented, compared with those obtained for the case of a constant-density plasma, while future developments and conclusions are briefly discussed in the last section.

Manuscript received July 28, 1997; revised February 20, 1998.

R. Borghi is with the Dipartimento di Ingegneria Elettronica, Università degli Studi "Roma Tre," I-00146, Rome, Italy.

F. Frezza, G. Gerosa, C. Santini, and G. Schettini are with the Dipartimento di Ingegneria Elettronica, Università degli Studi "La Sapienza," I-00184, Rome, Italy (e-mail: schettini@die.ing.uniroma1.it).

M. Santarsiero is with the Dipartimento di Fisica, Università degli Studi "Roma Tre," I-00146, Rome, Italy.

Publisher Item Identifier S 0093-3813(98)06374-7.

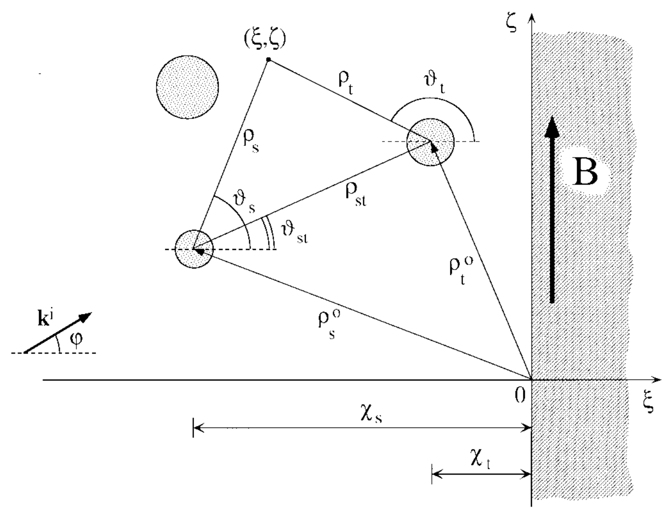

Fig. 1. Geometry of the scattering problem.

II. Theoretical Analysis

A. Solution of the Scattering Problem

The problem under investigation is the scattering of an electromagnetic, linearly polarized plane wave, with wavevector $\mathbf{k}^i$, impinging on a group of perfectly conducting parallel cylinders placed near a plane plasma surface, parallel to the cylinders (see Fig. 1). φ is the angle between the wavevector $\mathbf{k}^i$ and the direction perpendicular to the surface, and thus $\mathbf{k}^i$ is related to φ through the expressions

$$\begin{aligned} k_{\|}^i &= k_0 \sin\varphi \\ k_{\perp}^i &= k_0 \cos\varphi \end{aligned} \tag{1}$$

where the symbols $\|$ and $\perp$ refer to the parallel and orthogonal component of a vector with respect to the interface, respectively. The interface is described by its complex reflection coefficient $\Gamma(n_{\|})$, where $\mathbf{n} = (n_{\perp}, n_{\|}) = \mathbf{k}/k_0$, $\mathbf{k}$ being the wavevector of a typical plane wave impinging on the surface and k_0 the vacuum wavenumber. The structure is assumed to be infinite in the y direction, so that the problem can be considered as two-dimensional. Since the toroidal confinement magnetic field inside the plasma $\mathbf{B}$ is assumed to be parallel to the ζ-axis, the linear polarization with the magnetic vector parallel to the axes of the cylinders (H polarization) has been chosen to properly launch a lower hybrid slow wave [2]. In the following, for brevity, dimensionless coordinates $\xi = k_0 x$, $\zeta = k_0 z$ will be used. Let $\boldsymbol{\rho}_t^0 \equiv (\xi_t^0, \zeta_t^0)$ $(t = 1, \cdots, N)$ be the position vector of the axis of the tth cylinder in the main reference frame $(O\xi\zeta)$ (*MRF* from now on) and $\boldsymbol{\rho}_t \equiv (\xi_t, \zeta_t)$ $(t = 1, \cdots, N)$ be the typical position vector in the frame centered on that cylinder (*RF*$_t$ from now on). It is convenient to choose the ζ-axis of *MRF* lying on the plasma surface.

To obtain the solution in the absence of the interface [12], it is customary to expand the diffracted field in terms of cylindrical functions, each one given by the product of the Hankel function of integer order times the angular factor $\exp(in\vartheta)$. The expansion coefficients can be determined by imposing the electromagnetic boundary conditions on the conducting cylinders: to this aim it is convenient to express the field in terms of cylindrical functions centered on the axes of the cylinders.

In the presence of a plane surface, owing to the various geometrical features of the interacting waves and bodies, the imposition of the boundary conditions is a quite difficult task. In particular, since the reflection properties of a plane of discontinuity for the electromagnetic constants are generally known for incident plane waves [12], to obtain the rigorous solution it is essential to use the analytical plane-wave expansion of the above mentioned cylindrical functions [13]. In the following of the present subsection we give a brief report of the analysis developed in [11].

It is convenient to express the magnetic field $\mathcal{H}_{\text{tot}}$ as the sum of the following fields:

- $\mathcal{H}_i$: field of the incident plane wave;
- $\mathcal{H}_r$: field due to the reflection of $\mathcal{H}_i$ by the plane surface;
- $\mathcal{H}_d$: field scattered from the cylinders;
- $\mathcal{H}_{dr}$: field due to the reflection of $\mathcal{H}_d$ by the plane surface.

By using the expression of a plane wave in terms of Bessel functions of the first kind [14], for the incident field we get

$$\begin{aligned} \mathcal{H}_i(\xi,\zeta) &= \mathcal{H}_0 \exp\Big(in_{\perp}^i \xi_t^0 + in_{\|}^i \zeta_t^0\Big) \exp\Big(in_{\perp}^i \xi_t + in_{\|}^i \zeta_t\Big) \\ &= \mathcal{H}_0 \exp\Big(in_{\perp}^i \xi_t^0 + in_{\|}^i \zeta_t^0\Big) \sum_{m=-\infty}^{+\infty} i^m \exp(-im\varphi) \\ &\quad \times J_m(\rho_t) \exp(im\vartheta_t) \end{aligned} \tag{2}$$

where $\mathcal{H}_0$ is the amplitude of the incident plane wave and (ρ_t, ϑ_t) are polar coordinates in *RF*$_t$. Equation (2) represents the incident field evaluated at the point having coordinates (ξ, ζ) in *MRF* as a function of the coordinates (ξ_t, ζ_t) in *RF*$_t$. With a similar procedure, the field $\mathcal{H}_r$ takes the form

$$\begin{aligned} \mathcal{H}_r(\xi,\zeta) &= \mathcal{H}_0 \Gamma\Big(n_{\|}^i\Big) \exp\Big(-in_{\perp}^i \xi_t^0 + in_{\|}^i \zeta_t^0\Big) \\ &\quad \times \exp\Big(-in_{\perp}^i \xi_t + in_{\|}^i \zeta_t\Big) \\ &= \mathcal{H}_0 \Gamma\big(n_{\|}^i\big) \exp\Big(-in_{\perp}^i \xi_t^0 + in_{\|}^i \zeta_t^0\Big) \\ &\quad \times \sum_{m=-\infty}^{+\infty} i^m \exp(-im\bar{\varphi})\, J_m(\rho_t) \exp(im\vartheta_t) \end{aligned} \tag{3}$$

where $\bar{\varphi} = \pi - \varphi$ denotes the propagation angle of the reflected plane wave.

The field $\mathcal{H}_d$ is given in terms of a superposition of cylindrical functions weighted with unknown coefficients c_{sm} $(s = 1, \cdots, N; m = 0, \pm 1, \pm 2 \cdots)$, i.e.,

$$\mathcal{H}_d(\xi,\zeta) = \mathcal{H}_0 \sum_{s=1}^{N} \sum_{m=-\infty}^{+\infty} i^m \exp(-im\varphi) c_{sm}\, \mathrm{CW}_m(\xi_s, \zeta_s) \tag{4}$$

where $\mathrm{CW}_m(\xi_s, \zeta_s)$ is the cylindrical function

$$\mathrm{CW}_m(\xi_s, \zeta_s) = H_m^{(1)}(\rho_s) \exp(im\vartheta_s) \tag{5}$$

and $H_m^{(1)}$ is the outgoing Hankel function [14].

After some algebraic manipulations, we can write $\mathcal{H}_d$ as follows:

$$\begin{aligned} \mathcal{H}_d(\xi,\zeta) &= \mathcal{H}_0 \sum_{m=-\infty}^{+\infty} J_m(\rho_t) \exp(im\vartheta_t) \\ &\quad \times \sum_{s=1}^{N} \sum_{\ell=-\infty}^{+\infty} i^{\ell} \exp(-i\ell\varphi)\, c_{s\ell} \\ &\quad \times \left[\mathrm{CW}_{\ell-m}(\xi_{st}, \zeta_{st})(1-\delta_{st}) + \delta_{st}\delta_{\ell m} \frac{H_m^{(1)}(\rho_t)}{J_m(\rho_t)} \right]. \end{aligned} \tag{6}$$

The interaction between the sth and tth cylinders is contained in the term $\mathrm{CW}_{\ell-m}(\xi_{st}, \zeta_{st})\,(1-\delta_{st})$ of (6), which is a consequence of Graf's formula [14], giving the expression of a cylindrical wave emitted by the sth cylinder in the *RF*$_t$. When all cylinders can be considered as noninteracting, due to the vanishing of the interaction term, the field (6) reduces to the superposition of N fields evaluated by means of the classical formula for an isolated cylinder [12]. For example, this happens when the mutual distances between the cylinders are large enough, owing to the behavior of the Hankel functions [14].

The last term $\mathcal{H}_{dr}$ can be obtained starting from (4) and introducing the plane-wave spectrum of the cylindrical functions (5), defined as

$$F_m(\xi, n_{\|}) = \int_{-\infty}^{+\infty} \mathrm{CW}_m(\xi,\zeta) \exp\left(-in_{\|}\zeta\right) d\zeta. \tag{7}$$

In [13] and [15] the analytical expression of the function F_m was derived, yielding

$$F_m(\xi, n_\|) = \frac{2\exp(in_\perp \xi)}{n_\perp} \exp(-im \arccos n_\|), \quad n_\| \in (-\infty, +\infty). \tag{8}$$

By the knowledge of the spectrum $F_m(\xi, n_\|)$, the field $\mathcal{H}_{dr}$ takes the form

$$\mathcal{H}_{dr}(\xi, \zeta) = \mathcal{H}_0 \sum_{s=1}^{N} \sum_{m=-\infty}^{+\infty} i^m \exp(-im\varphi)\, c_{sm} \times \mathrm{RW}_m(2\chi_s - \xi_s, \zeta_s) \tag{9}$$

where the function $\mathrm{RW}_m(\xi, \zeta)$ is

$$\mathrm{RW}_m(\xi, \zeta) = \frac{1}{2\pi} \int_{-\infty}^{+\infty} \Gamma(n_\|)\, F_m(\xi, n_\|) \exp(in_\| \zeta)\, dn_\|. \tag{10}$$

Equation (9) shows that $\mathcal{H}_{dr}$ can be thought of as the superposition of the fields diffracted by "image" cylinders centered at the points $(-\xi_s^0, \zeta_s^0)$, for $s = 1, \cdots, N$. These fields are modulated by the presence of the interface [see (10)].

Finally, by using (9) and (10), it is possible to show that $\mathcal{H}_{dr}$ can be expanded in RF_t as follows:

$$\mathcal{H}_{dr}(\xi, \zeta) = \mathcal{H}_0 \sum_{m=-\infty}^{+\infty} J_m(\rho_t) \exp(im\vartheta_t) \times \sum_{s=1}^{N} \sum_{\ell=-\infty}^{+\infty} i^\ell \exp(-i\ell\varphi)\, c_{s\ell} \times \mathrm{RW}_{\ell+m}(\chi_s + \chi_t, \zeta_t^0 - \zeta_s^0). \tag{11}$$

If the cylinders were far enough from the plasma surface, the field (11) could be neglected. This is taken into account by the fact that the $\mathrm{RW}_{\ell+m}$ functions vanish for large values of the first argument, as can be seen starting from their definition [see (10)]. In the following, however, due to the small distance between plasma and scatterers, we will not use such an approximation.

Once all the contributions to the total field have been written in RF_t, we can easily impose the boundary conditions, which, on each cylinder surface, assume the form

$$\partial_{\rho_t} \mathcal{H}_{\mathrm{tot}}|_{\rho_t = k_0 a_t} = 0 \quad (t = 1, \cdots, N). \tag{12}$$

By substituting from (2), (3), (6), and (11) into (12), after some algebra we obtain the following linear system for the unknown coefficients

$$\sum_{s=1}^{N} \sum_{\ell=-\infty}^{+\infty} A_{m\ell}^{st} c_{s\ell} = B_m^t, \quad \begin{pmatrix} m = 0, \pm 1, \pm 2, \cdots \\ t = 1, \cdots, N \end{pmatrix} \tag{13}$$

where

$$A_{m\ell}^{st} = i^\ell \exp(-i\ell\varphi)\big\{\big[\mathrm{CW}_{\ell-m}(\xi_{st}, \zeta_{st})(1 - \delta_{st}) + I_{\ell+m}^{st}\big] G_m(k_0 a_t) + \delta_{st}\delta_{\ell m}\big\} \tag{14}$$

$$I_p^{st} = \mathrm{RW}_p(\chi_s + \chi_t, \zeta_t^0 - \zeta_s^0) \tag{15}$$

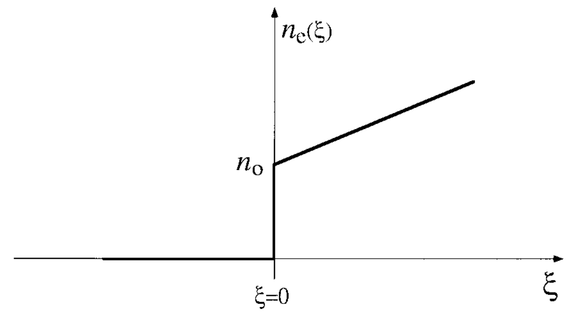

Fig. 2. Behavior of the plasma density.

$$B_m^t = -i^m \exp\big(in_\|^i \zeta_t^0\big) G_m(k_0 a_t) \times \big[\exp\big(in_\perp^i \xi_t^0\big) \exp(-im\varphi) + \Gamma\big(n_\|^i\big) \exp\big(-in_\perp^i \xi_t^0\big) \exp(-im\bar{\varphi})\big] \tag{16}$$

and the function $G_m(\rho)$ is defined as

$$G_m(\rho) = \frac{J_m'(\rho)}{H_m^{(1)\prime}(\rho)} \tag{17}$$

where the prime denotes derivation.

B. The Reflection Coefficient

The external layer of a tokamak plasma is quite well approximated by a cold plasma of a linearly increasing density [2], [8], [9]. Therefore, with reference to Fig. 2, we assume the following functional form of the electron density $n_e(\xi)$:

$$n_e(\xi) = \begin{cases} 0 & \xi < 0 \\ n_0 + \Delta\xi & \xi > 0 \end{cases} \tag{18}$$

where n_0 accounts for a possible density discontinuity and Δ is the density increase for normalized unit length.

In order to calculate the reflection coefficient of the plasma surface, it is important to know the plasma admittance [6]

$$Y_{\mathrm{pl}}(n_\|) = -\frac{\mathcal{H}_y^{\mathrm{pl}}(\xi = 0; n_\|)}{\mathcal{E}_z^{\mathrm{pl}}(\xi = 0; n_\|)}. \tag{19}$$

Once this admittance is known, the reflection coefficient $\Gamma(n_\|)$ is determined by means of the following [6]:

$$\Gamma(n_\|) = \frac{1 - \eta(n_\|)}{1 + \eta(n_\|)} \tag{20}$$

where

$$\eta(n_\|) = \frac{Y_{\mathrm{pl}}(n_\|)}{Y_0} \sqrt{1 - n_\|^2} \tag{21}$$

is the normalized plasma admittance and Y_0 is the vacuum admittance.

To evaluate $Y_{\mathrm{pl}}(n_\|)$ we start from the wave equation for the electric field component in the plasma $\mathcal{E}_z^{\mathrm{pl}}$, i.e., [2], [8]

$$\frac{\partial^2 \mathcal{E}_z^{\mathrm{pl}}(\xi)}{\partial \xi^2} + \left(1 - \frac{n_e(\xi)}{n_c}\right)(1 - n_\|^2)\mathcal{E}_z^{\mathrm{pl}}(\xi) = 0 \tag{22}$$

where n_c is the cutoff density of the plasma [8]. The magnetic field component $\mathcal{H}_y^{\rm pl}$ is deducible from the following:

$$\mathcal{H}_y^{\rm pl}(\xi) = \frac{iY_0}{\left(1-n_\parallel^2\right)} \frac{\partial \mathcal{E}_z^{\rm pl}(\xi)}{\partial \xi} \tag{23}$$

and is therefore known once $\mathcal{E}_z^{\rm pl}$ is available.

$Y_{\rm pl}(n_\parallel)$ assumes different expressions in the two ranges $|n_\parallel| < 1$, i.e., a homogeneous incident wave on the vacuum side, and $|n_\parallel| > 1$, corresponding to an evanescent incident wave on the vacuum side. Therefore, we consider each case individually.

Homogeneous Incident Waves: $|n_\parallel| < 1$. Equation (22) can be written as

$$\frac{\partial^2 \mathcal{E}_z^{\rm pl}(\xi)}{\partial \xi^2} - \left(1-n_\parallel^2\right)\frac{\Delta}{n_c}(\xi-\xi_c)\mathcal{E}_z^{\rm pl}(\xi) = 0 \tag{24}$$

where

$$\xi_c = \frac{n_c - n_0}{\Delta} < 0. \tag{25}$$

ξ_c is a negative quantity because n_0 must be greater than n_c to allow propagation of the lower hybrid plasma wave. By introducing the quantities

$$w = \gamma^{1/3}(\xi - \xi_c) > 0 \tag{26}$$

$$\gamma = \frac{\Delta}{n_c}\left(1-n_\parallel^2\right) > 0 \tag{27}$$

(24) turns into

$$\frac{\partial^2 F(w)}{\partial w^2} - wF(w) = 0 \tag{28}$$

where

$$F(w) = \mathcal{E}_z^{\rm pl}(\gamma^{-1/3}w + \xi_c). \tag{29}$$

Equation (28) is the Airy equation. Its general solution may be written as a linear combination of the two independent Airy functions $\mathrm{Ai}(w)$, $\mathrm{Bi}(w)$, as follows [16]:

$$F(w) = a\mathrm{Ai}(w) + b\mathrm{Bi}(w) \tag{30}$$

a and b being two complex constants. By recalling the relationship between w and the spatial coordinate ξ [see (26)] and considering that

$$\lim_{w\to\infty} \mathrm{Bi}(w) = +\infty \tag{31}$$

we note that b must vanish in order to obtain physically significant solutions. Therefore, in particular, we get

$$\mathcal{E}_z^{\rm pl}(0) = a\mathrm{Ai}(w_0) \tag{32}$$

and, from (23)

$$\mathcal{H}_y^{\rm pl}(0) = iaY_0\left(\frac{\Delta}{n_c}\right)^{1/3}\left(1-n_\parallel^2\right)^{-2/3}\mathrm{Ai}'(w_0) \tag{33}$$

where

$$w_0 = w|_{\xi=0} = -\gamma^{1/3}\xi_c > 0. \tag{34}$$

By using (32) and (33) together with (19) and (21), the following normalized plasma admittance is obtained:

$$\eta(n_\parallel) = -i\left(\frac{\Delta}{n_c}\right)^{1/3}\left(1-n_\parallel^2\right)^{-1/6}\frac{\mathrm{Ai}'(w_0)}{\mathrm{Ai}(w_0)}. \tag{35}$$

Evanescent Incident Waves: $|n_\parallel| > 1$. In this case (22) turns into

$$\frac{\partial^2 \mathcal{E}_z^{\rm pl}(\xi)}{\partial \xi^2} + \left(n_\parallel^2 - 1\right)\frac{\Delta}{n_c}(\xi-\xi_c)\mathcal{E}_z^{\rm pl}(\xi) = 0. \tag{36}$$

By proceeding as in the previous case we get the Airy equation in the following form:

$$\frac{\partial^2 F(w)}{\partial w^2} + wF(w) = 0 \tag{37}$$

provided that γ in (26) is now defined as

$$\gamma = \frac{\Delta}{n_c}\left(n_\parallel^2 - 1\right) > 0. \tag{38}$$

Owing to the positive sign in front of the second term in (37), we have to consider solutions of the form

$$F(w) = a\mathrm{Ai}(-w) + b\mathrm{Bi}(-w). \tag{39}$$

In order to determine the constants a and b, it is useful to consider $\mathcal{E}_z^{\rm pl}(\xi)$ at very large ξ values. In this limit the Airy functions can be substituted by their asymptotic expansions [16] allowing us to write

$$\begin{aligned}\mathcal{E}_z^{\rm pl}(\xi) = F(w) &\sim \pi^{-1/2}w^{-1/4}b \\ &\times \left[\frac{a}{b}\sin\left(w+\frac{\pi}{4}\right) + \cos\left(w+\frac{\pi}{4}\right)\right].\end{aligned} \tag{40}$$

To obtain from the previous equation a pure plane wave, we have to choose the ratio a/b equal to $\pm i$. Consequently

$$\mathcal{E}_z^{\rm pl}(\xi) \sim \pi^{-1/2}w^{-1/4}b\exp\left[\pm i\left(w+\frac{\pi}{4}\right)\right]. \tag{41}$$

It is possible to remove the ambiguity in the sign of a/b by computing the ξ component, say P_ξ, of the Poynting vector relevant to the field (40).
After some algebra we achieve the following:

$$P_\xi = \frac{1}{2\pi}Y_0\left(\frac{\Delta}{n_c}\right)^{1/3}\left(1-n_\parallel^2\right)^{-2/3}\mathrm{Im}(a^*b) \tag{42}$$

where $\mathrm{Im}(\cdot)$ denotes the imaginary part. By choosing $a/b = -i$, P_ξ is positive and the real power flow is in the positive ξ direction, corresponding to a net energy transmission from vacuum into the plasma. Therefore, the field (39) must be of the form

$$\mathcal{E}_z^{\rm pl}(\xi) = a[\mathrm{Ai}(-w) + i\mathrm{Bi}(-w)]. \tag{43}$$

We note that this choice corresponds to a negative phase velocity [see (41)] and then the wave is backward [17]. Consequently, the relevant normalized plasma admittance turns out to be

$$\eta(n_\parallel) = \left(\frac{\Delta}{n_c}\right)^{1/3}\left(1-n_\parallel\right)^{-1/6}\frac{\mathrm{Ai}'(-w_0) + i\mathrm{Bi}'(-w_0)}{\mathrm{Ai}(-w_0) + i\mathrm{Bi}(-w_0)} \tag{44}$$

where w_0 has the expression (34) and γ is given in (38).

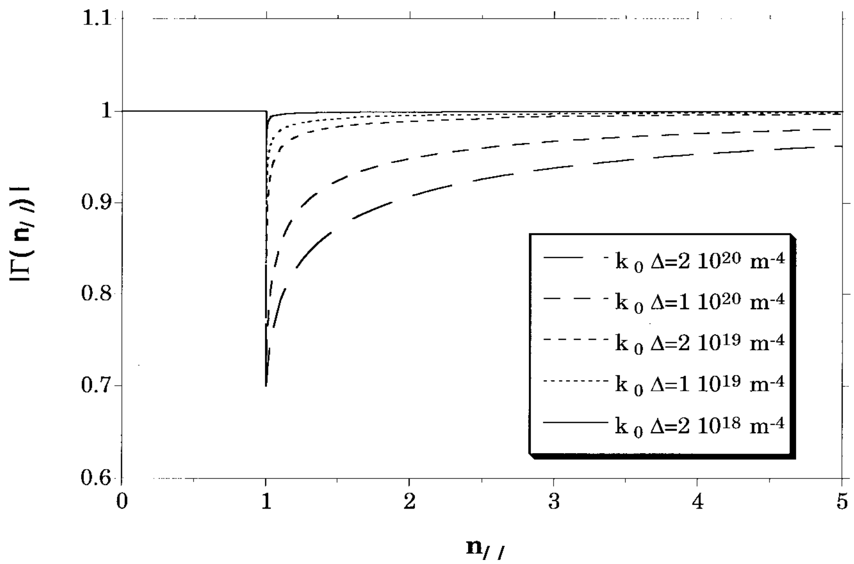

Fig. 3. Plot of $|\Gamma(n_{||})|$, $n_0/n_c = 2$, $f = 10$ GHz.

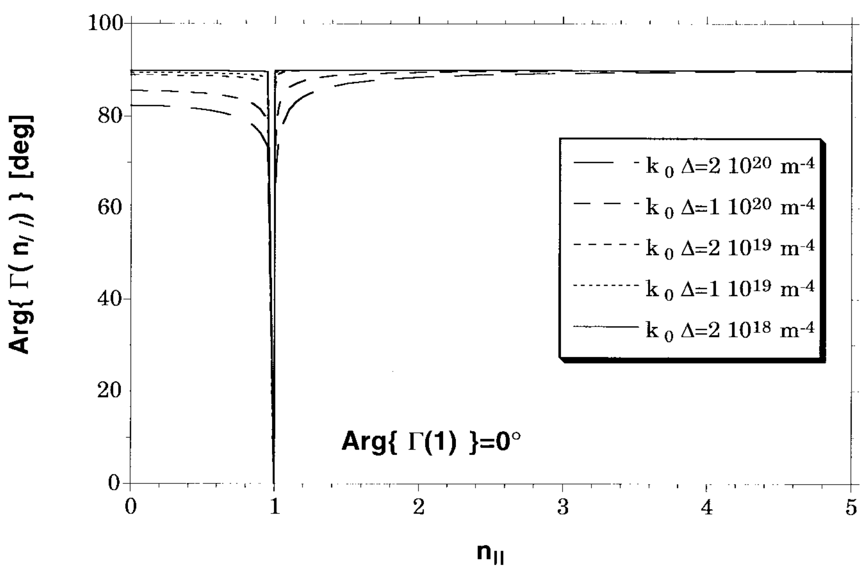

Fig. 4. Phase of $\Gamma(n_{||})$, $n_0/n_c = 2$, $f = 10$ GHz.

The reflection coefficient in (20) assumes different forms in the aforementioned two ranges. In particular, when $|n_{||}| < 1$ we have to use (35) for η, while for $|n_{||}| > 1$ (44) holds.

By considering the limit of small Δ values, the present approach gives the following result for the reflection coefficient:

$$\Gamma_0 = \frac{1 - i\sqrt{\frac{n_0}{n_c} - 1}}{1 + i\sqrt{\frac{n_0}{n_c} - 1}}. \tag{45}$$

This expression coincides with that obtained for a constant density plasma [6], [9], as expected.

In Fig. 3 several plots of $|\Gamma(n_{||})|$ are shown. The curves refer to a density ratio $n_0/n_c = 2$. All the graphs reported in the following present several curves, referring to different $k_0\Delta$ values in the range $k_0\Delta \in [2\times 10^{18}\ \mathrm{m}^{-4}, 2\times 10^{20}\ \mathrm{m}^{-4}]$. As expected, $|\Gamma| = 1$ for $|n_{||}| < 1$, giving total reflection for a homogeneous wave propagating in a vacuum. Moreover, as Δ decreases, the behavior of $|\Gamma|$ approaches the value $|\Gamma_0|$ predicted by the constant-density model [see (45)].

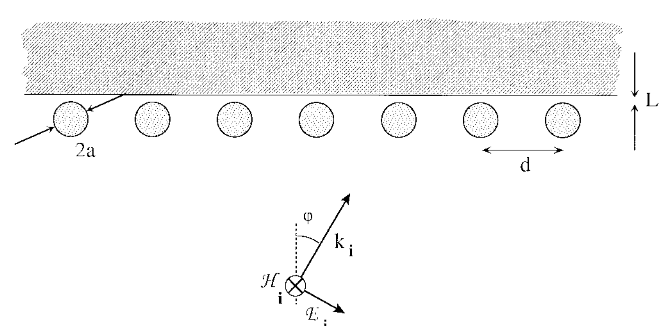

Fig. 5. Single-layered quasi-optical grill.

In Fig. 4 several plots of the phase of $\Gamma(n_{||})$ are shown for the same values as before. As $k_0\Delta \to 0$, the phase approaches

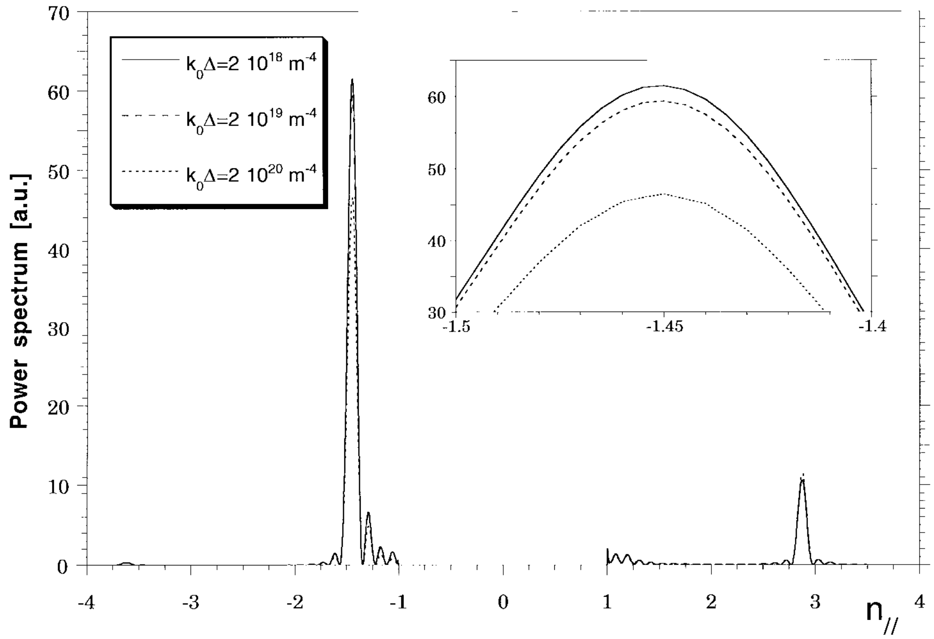

Fig. 6. Coupled power spectra for the structure of Fig. 5 for different values of $k_0\Delta$ and $N = 20$, $k_0 a = 0.85$, $k_0 L = 0.25$, $\varphi = 45°$, $n_0/n_c = 2$, $k_0 d = 2.9$, and $f = 10$ GHz.

$\pi/2$, matching the constant-density model results. Details on the computation of $\Gamma(n_{||})$ are given in the Appendix.

III. Numerical Results

In this section we make reference to the structure analyzed in [6], [18], and [19]. First, we give some results pertinent to the layout shown in Fig. 5: a single-layer quasi-optical grill of perfectly conducting circular cylinders placed in front of the plasma surface.

Fig. 6 shows the obtained coupled-power spectra for different values of the density slope $k_0\Delta$. It can be seen that the peak value of the -1 order increases on decreasing $k_0\Delta$ and for $k_0\Delta \leq 2\times10^{18}$ m^{-4} the spectrum is practically coincident with that obtained in the case of a constant-density plasma (see [6, Fig. 4]). From a quick sight to the spectra shapes we expect a worsening of the coupling parameters when the density slope increases, as will be confirmed by the results we are going to present.

In Fig. 7 we report plots of the reflected power [6] as a function of the number N of cylinders in the grill for different density slopes. As expected, when the density slope increases, the coupling is seen to become worse, and approaches the results given in ([6, Fig. 5]) when $k_0\Delta$ is less than 2×10^{18} m^{-4}.

In Fig. 8, the directivity, defined as the ratio between the power coupled for negative values of $n_{||}$ and the total coupled power, is plotted versus N for several $k_0\Delta$ values. Also in this case the results are consistent with those in [6] for the case $k_0\Delta = 0$ and become worse for increasing slopes. The dependence of both the coupling parameters on the plasma density for an array of $N = 10$ cylinders is reported in Figs. 9 and 10, respectively.

A different layout, consisting in a layer of pairs of contacting cylinders, is sketched in Fig. 11. For this structure we present, in Figs. 12 and 13, curves of reflected power and directivity versus the tilting angle α. Analogous comments as for the previous Figs. 7 and 8 apply in this case.

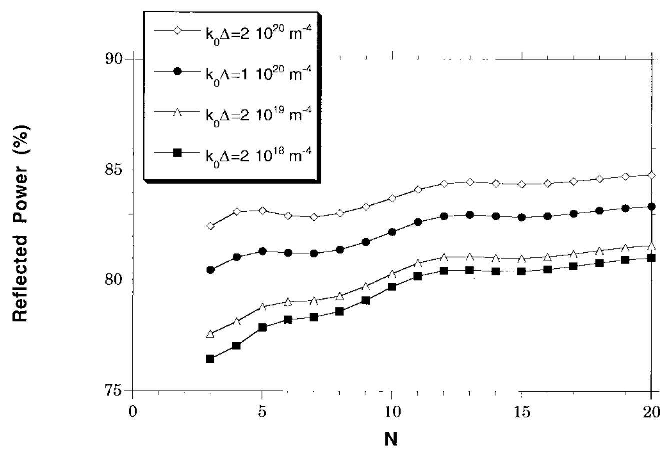

Fig. 7. Reflected power (%) versus number of cylinders N; $k_0 a = 0.85$, $k_0 L = 0.25$, $\varphi = 45°$, $n_0/n_c = 2$, $k_0 d = 2.9$, and $f = 10$ GHz.

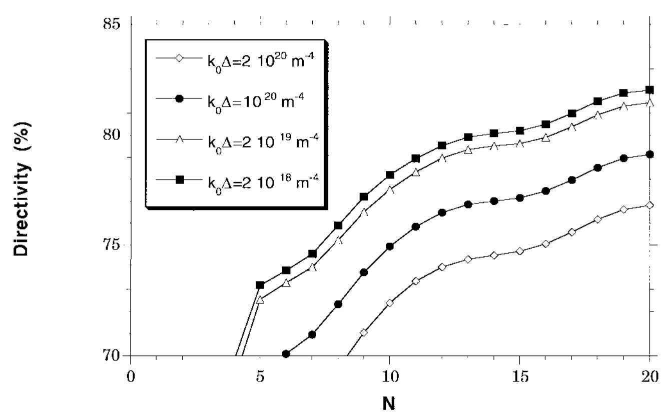

Fig. 8. Directivity (%) for the same case of Fig. 7.

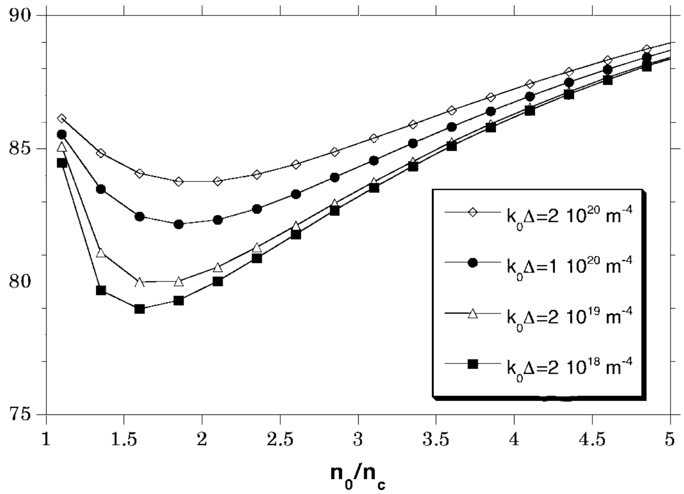

Fig. 9. Reflected power (%) versus normalized density n_0/n_c; $N = 10$, $k_0a = 0.85$, $k_0d = 2.9$, $k_0L = 0.25$, $\varphi = 45°$, and $f = 10$ GHz.

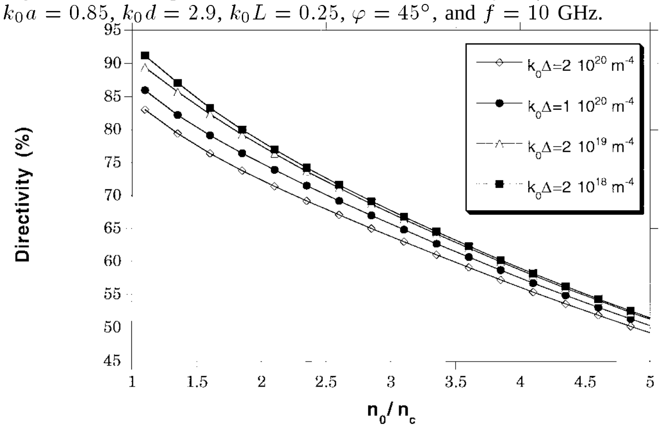

Fig. 10. Directivity (%) versus n_0/n_c. The other parameters are the same as in Fig. 9.

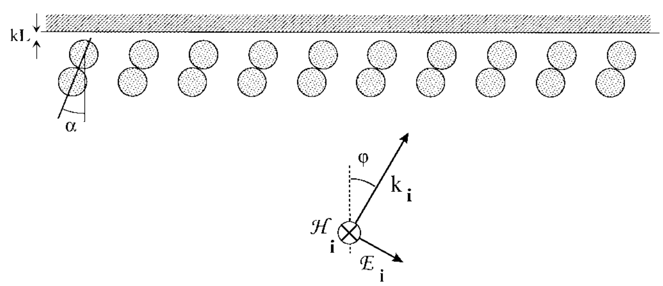

Fig. 11. Array of pairs of cylinders.

A more efficient configuration has been proposed in [18] and [19] for a Gaussian beam illumination and a constant-density plasma. A consistent analysis for that configuration and for a plasma density of the kind considered in this paper can be performed once an incident Gaussian beam is assumed. This problem is an extension of the present method and its analysis is in progress.

IV. Conclusions

In this paper, we have shown the effects of a quite realistic model for the external layer of a thermonuclear plasma on the coupling parameters (reflected power and directivity) when a quasi-optical grill of conducting circular cylinders is used

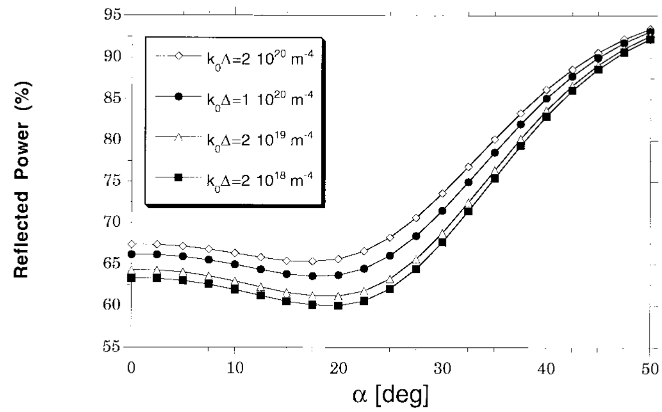

Fig. 12. Reflected power (%) versus α of an array of ten pairs of cylinders, $k_0a = 0.85$, $k_0d = 2.9$, $k_0L = 0.25$, $\varphi = 25°$, $n_0/n_c = 2$, $f = 10$ GHz.

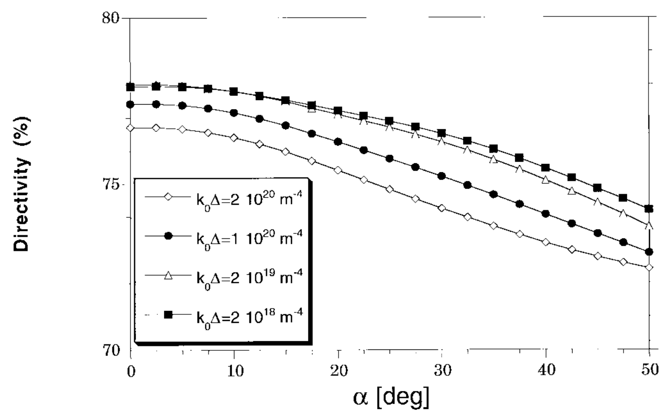

Fig. 13. Directivity (%) versus α for the same case of Fig. 12.

to launch lower-hybrid slow plasma waves. Such a model considers that the electron density, versus the distance from the plasma surface, behaves like a step followed by a linear ramp.

The analytical and computational difficulties arisen, with respect to the constant-density case, have been discussed and overcome. Numerical results have been presented for the coupling parameters for various geometrical configurations and physical parameters. Such results have shown to tend to the ones pertinent to the constant-density case when the slope of the ramp tends to zero.

As a general remark, we have found that the performances of the coupler become systematically worse on increasing the plasma density slope, so that the values of the coupled power and directivity are generally lower than those evaluated by modeling the plasma density as a constant.

The analysis could be extended to the case of an incident Gaussian beam, representing a more realistic model for the incident field. This could be performed by means of a suitable plane-wave representation of the Gaussian beam, following the lines of [18], [19]. Furthermore, the more efficient configurations proposed in the latter references could be profitably analyzed for the case of a plasma with linearly increasing density, when an incident Gaussian beam is considered. Finally better performances may be obtained using a systematic optimization procedure or employing scattering elements of noncircular cross sections, such as elliptical [9]

$$\eta(n_{\|}) \approx \begin{cases} i\sqrt{\frac{1}{w_0}\left(\frac{n_0}{n_c}-1\right)}\frac{\sum_{k=0}^{\infty}(-1)^k d_k z_0^{-k}}{\sum_{k=0}^{\infty}(-1)^k c_k z_0^{-k}} & |n_{\|}|<1 \\ \sqrt{\frac{1}{w_0}\left(\frac{n_0}{n_c}-1\right)}\frac{\sum_{k=0}^{\infty}(-1)^{2k} d_{2k} z_0^{-2k}+i\sum_{k=0}^{\infty}(-1)^{2k+1} d_{2k+1} z_0^{-(2k+1)}}{\sum_{k=0}^{\infty}(-1)^{2k} c_{2k} z_0^{-2k}+i\sum_{k=0}^{\infty}(-1)^{2k+1} c_{2k+1} z_0^{-(2k+1)}} & |n_{\|}|>1 \end{cases} \tag{49}$$

or rectangular [20], [21] ones. The limits of applicability of our method do not differ much from the ones given in [2] where a similar problem was faced for a waveguide grill launcher. In particular, the effect of the plasma curvature should be taken into account, adapting the presented model to the various tokamaks making use of suitable approximations. Our approach can be easily extended to the case of an obliquely incident plane wave with respect to the cylinder axes, and this is the key to generalize the technique to the case of finite height cylinders by means of a suitable Fourier expansion (with respect to the y-direction).

Finally, as is well known, the plasma density undergoes random fluctuations which are usually neglected. A future goal of our work is to include these effects using statistical methods.

APPENDIX
NUMERICAL COMPUTATION OF $\Gamma(n_{\|})$

The computation of the Airy functions for values of $k_0\Delta$ greater than 10^{19} m^{-4} can be performed by using their relation with the Bessel functions of fractional order or, alternatively, their expansion in ascending series [16]. These techniques are very efficient and their implementation does not present numerical difficulties.

For smaller values of $k_0\Delta$, the asymptotic expansions of Ai, Ai$'$, Bi, and Bi$'$ may be used [16]. However, such expansions give rise to loss of precision in the limit $\Delta \to 0$. Nevertheless, it is important to verify that in such limit the linear density plasma model results match those obtained for the constant density one. To this aim, it is possible to obtain different forms for (35) and (44), which allow an easy and fast computation of the $\Gamma(n_{\|})$ function for very small values of $k_0\Delta$. In particular, we note that

$$\lim_{\Delta\to 0} w_0 = +\infty. \tag{46}$$

Thus, the asymptotic form for $\Gamma(n_{\|})$ with Δ approaching zero may be obtained from the expansion of (35) and (44) for large values of w_0. It is useful, therefore, to express (35) and (44) as functions of w_0 only. From (27), (34), and (38), in both cases $|n_{\|}|<1$ and $|n_{\|}|>1$, we get

$$\left(\frac{\Delta}{n_c}\right)^{1/3} = \sqrt{\frac{1}{w_0}\left(\frac{n_0}{n_c}-1\right)}\left|1-n_{\|}^2\right|^{1/6}. \tag{47}$$

Substituting (47) into (35) and (44), we obtain

$$\eta(n_{\|}) = \begin{cases} -i\sqrt{\frac{1}{w_0}\left(\frac{n_0}{n_c}-1\right)}\frac{\mathrm{Ai}'(-w_0)}{\mathrm{Ai}(-w_0)} & |n_{\|}|<1 \\ \sqrt{\frac{1}{w_0}\left(\frac{n_0}{n_c}-1\right)}\frac{\mathrm{Ai}'(-w_0)+i\mathrm{Bi}'(-w_0)}{\mathrm{Ai}(-w_0)+i\mathrm{Bi}(-w_0)} & |n_{\|}|>1. \end{cases} \tag{48}$$

By using the asymptotic expansions of the Airy functions [16] for large arguments, (48) in the limit $\Delta \to 0$, turns into (49) shown at the top of the page where

$$z_0 = \frac{2}{3}w_0^{3/2} \tag{50}$$

and

$$\begin{cases} c_0 = 1 \\ c_k = \frac{(2k+1)(2k+3)\cdots(6k-1)}{216^k k!} \end{cases} \quad \begin{cases} d_0 = 1 \\ d_k = -\frac{(6k+1)}{(6k-1)} \end{cases} \quad (k=1,2,\cdots). \tag{51}$$

By substituting the η values of (49) into (20) the expressions of the reflection coefficient $\Gamma(n_{\|})$ are easily obtained. Numerical tests have proved that this procedure is very efficient, accurate, and reliable in a wide range of Δ values.

REFERENCES

[1] R. A. Cairns, *Radiofrequency Heating of Plasmas*. Bristol, U.K.: Adam Hilger, 1991, ch. 4.

[2] M. Brambilla, "Slow-wave launching at the lower hybrid frequency using a phased waveguide array," *Nucl. Fusion*, vol. 16, no. 1, pp. 47–54, 1976.

[3] C. Gormezano, P. Briand, G. Briffod, G. T. Hoang, T. K. N'Guyen, D. Moreau, and G. Rey, "Lower-hybrid plasma heating via a new launcher: The multijunction grill," *Nucl. Fusion*, vol. 25, no. 4, pp. 419–423, 1985.

[4] P. Schild, C. Gormezano, M. Pain, M. Brusati, M. Cox, C. Gardner, T. Hender, R. Lewis, and B. Lloyd, "Numerical simulation of the hyperguide transmission properties," presented at the *Eur. Workshop LH Heating Current Drive, JET*, Abingdon, U.K., 1992.

[5] M. I. Petelin and E. Suvorov, "Quasi-optical grill for excitation of lower hybrid waves in a toroidal plasma," *Sov. Tech. Phys. Lett.*, vol. 15, no. 11, pp. 882–883, 1989.

[6] F. Frezza, G. Schettini, F. Gori, M. Santarsiero, and F. Santini, "Quasi-optical launchers for lower hybrid waves: A full wave approach," *Nucl. Fusion*, vol. 34, no. 9, pp. 1239–1246, 1994.

[7] J. P. Crenn and P. Bibet, "Quasi-optical grill using diffraction gratings for lower-hybrid wave systems," Assoc. Euratom-CEA, Centre d'Etudes de Cadarache, Saint Paul-lez-Durance, France, Rep. Eur. CEA-FC-1508, Aug. 1994.

[8] J. Stevens, M. Ono, R. Horton, and J. R. Wilson, "Edge density profile effects for lower hybrid waveguide coupling," *Nucl. Fusion*, vol. 21, no. 10, pp. 1259–1264, 1981.

[9] M. I. Petelin, E. V. Suvorov, N. F. Kovalev, S. E. Fil'chenkov, and A. I. Smirnov, "Quasi-optical diffraction grill for excitation of lower-hybrid waves in tokamaks," *Plasma Phys. Control. Fusion*, vol. 38, no. 5, pp. 593–610, 1996.

[10] L. Preinhaelter, "Quasi-optical grill mounted in hyperguide," *Nucl. Fusion*, vol. 36, no. 5, pp. 593–611, 1996.

[11] R. Borghi, F. Gori, M. Santarsiero, F. Frezza, and G. Schettini, "Plane-wave scattering by a set of perfectly conducting circular cylinders in the presence of a plane surface," *J. Opt. Soc. Amer. A*, vol. 13, no. 12, pp. 2441–2452, 1996.

[12] A. Ishimaru, *Electromagnetic Wave Propagation, Radiation and Scattering*. New York: Prentice-Hall, 1991, chs. 3, 11.

[13] G. Cincotti, F. Gori, M. Santarsiero, F. Frezza, F. Furnò, and G. Schettini, "Plane wave expansion of cylindrical functions," *Opt. Commun.*, vol. 95, no. 1, pp. 192–198, 1993.

[14] M. Abramowitz and I. Stegun, *Handbook of Mathematical Functions*. New York: Dover, 1972, ch. 9.

[15] R. Borghi, F. Frezza, F. Gori, M. Santarsiero, and G. Schettini, "Plane-wave scattering by a perfectly conducting circular cylinder near a plane surface: Cylindrical-wave approach," *J. Opt. Soc. Amer. A*, vol. 13, no. 3, pp. 483–493, 1996.

[16] M. Abramowitz and I. Stegun, *Handbook of Mathematical Functions*. New York: Dover, 1972, ch. 10.

[17] R. E. Collin, *Foundations for Microwave Engineering*, 2nd ed. Singapore: McGraw-Hill, 1992, p. 709.

[18] F. Frezza, G. Gerosa, F. Gori, M. Santarsiero, F. Santini, G. Schettini, and M. Sgroi, "Gaussian beam diffraction by a quasi-optical grating for coupling to lower-hybrid plasma waves," *Int. J. Infrared Millim. Waves*, vol. 16, no. 6, pp. 1009–1024, 1995.

[19] V. A. Avantaggiati, F. Frezza, G. Gerosa, G. Schettini, R. Borghi, and M. Santarsiero, "Gaussian beam excitation of quasioptical launchers for lower hybrid waves," *Nucl. Fusion*, vol. 37, no. 5, pp. 689–699, 1997.

[20] J. Preinhaelter, L. Vahala, and G. Vahala, "A new concept of launchers for lower-hybrid waves in tokamaks: Quasi-optical grills," in *Proc. Joint Varenna-Lausanne Workshop "Theory Fusion Plasmas,"* J. W. Connor, E. Sindoni, and J. Vaclavik, Eds. Varenna, Italy, Aug. 26–30, 1996, pp. 87–100.

[21] J. Preinhaelter, A. Coté, Y. Demers, V. Fuchs, L. Vahala, and G. Vahala, "Proposal of a quasi-optical grill operating at 3.7 GHz for TdeV tokamak," in *Proc. 24th EPS Conf. Control Fusion Plasma Phys.*, M. Schiffenhelm, R. Bartiromo, and F. Wagner, Eds. Berchtesgaden, Austria, June 9–13, 1997, pp. 309–312.

Riccardo Borghi received the *Laurea* degree in electronic engineering in 1991 and the Ph.D. degree in applied electromagnetics in 1997 from "La Sapienza" University of Rome, Italy.

In 1997 he joined the Department of Electronic Engineering of University "Roma Tre," Rome, Italy. His main interests are laser beam propagation, diffractive optics, scattering of electromagnetic and acoustic waves.

Fabrizio Frezza (S'87–M'92–SM'95) received the *Laurea* degree *cum laude* in electronic engineering in 1986 and the Ph.D. degree in applied electromagnetics in 1991 from "La Sapienza" University of Rome, Italy.

In 1986, he joined the Electronic Engineering Department of "La Sapienza" University of Rome where he has been a Researcher since 1990 and a temporary Professor of Electromagnetics since 1994. His main research activity concerns guiding structures, antennas and resonators for microwaves and millimeter waves, numerical methods, scattering, optical propagation, and plasma heating.

Dr. Frezza is a member of Sigma Xi, the Electrical and Electronic Italian Association (AEI), the Italian Society of Optics and Photonics (SIOF), and the Italian Society of Applied and Industrial Mathematics (SIMAI).

Giorgio Gerosa (A'58–LA'96) was born in Rome, Italy, in 1931. He graduated *cum laude* in electrical engineering at "La Sapienza" University of Rome, Italy, in 1956.

Since 1956, he has been with "La Sapienza" University of Rome where he has been engaged in teaching and research activities, and since 1967 he has been a full Professor of Microwaves and later of Electromagnetic Fields. Presently he is also Director of the Ph.D. course in applied electromagnetics and electrophysics sciences. His primary interests are in the propagation of electromagnetic waves in anisotropic media, in microwave hyperthermia for cancer therapy, in the analysis and design of microwave and millimeter-wave devices, and in the additional electromagnetic heating of a thermonuclear plasma for controlled fusion.

Dr. Gerosa is the Italian Official Member of Commission B (Fields and Waves) of URSI. He is also a member of the Electrical and Electronic Italian Association (AEI) and of the Italian Society of Applied and Industrial Mathematics (SIMAI).

Massimo Santarsiero received the *Laurea* degree in physics in 1988 and Ph.D. degree in applied electromagnetics in 1992 from "La Sapienza" University of Rome, Italy.

He worked at the Italian Energy and Environment Agency (ENEA) on holography and interferometry. Presently he is at the Department of Physics of the University "Roma Tre," Rome, Italy, where he works on optical coherence, laser beam characterization, electromagnetic scattering by microstructures.

Carlo Santini received the *Laurea* degree in electronic engineering in 1996 from "La Sapienza" University of Rome, Italy.

He presently collaborates with the Department of Electronic Engineering of "La Sapienza" University of Rome on electromagnetic scattering problems.

Giuseppe Schettini (S'84–M'96) received the *Laurea* degree in electronic engineering in 1986, the Ph.D. degree in applied electromagnetics and electrophysics sciences in 1991, and the *Laurea* degree in physics in 1995, all from "La Sapienza" University of Rome, Italy.

After his graduation in electronic engineering, he joined the Italian Energy and Environment Agency (ENEA) where he first worked on free electron lasers and then on the radiofrequency heating of thermonuclear plasmas. In 1992 he joined "La Sapienza" University of Rome as a Researcher and Assistant Professor of Electromagnetics. Since 1995 he has been a temporary Professor of Electromagnetic fields. His scientific activity is focused on radiofrequency heating of thermonuclear plasmas, ferrite resonators, propagation and diffraction of optical beams, diffractive optics, and free electron lasers.

Dr. Schettini is a member of the Italian Physical Society (SIF), the Italian Optics and Photonics Society (SIOF), "La Sapienza" unit of the Electromagnetics Group of Italian National Research Council (CNR), and "La Sapienza" unit of the Electronics CNR Group.